Contents list available at IJRED website

Int. Journal of Renewable Energy Development (IJRED)

Journal homepage: http://ejournal.undip.ac.id/index.php/ijred

Research Article

Performance Analysis of Flat-Plate and V-groove Solar Air Heater Through CFD Simulation

Debela Geneti Desisa[a], Gadisa Desa Shekata[b*]

[a]Faculty of Mechanical Engineering, Jimma Institute of Technology, Jimma University, Ethiopia

[b]Department of Mechanical Engineering, College of Engineering and Technology, Wolkite University, Ethiopia

ABSTRACT. The simplicity of solar flat plate air collector and free availability of solar energy sources attract attention to the optimization of the collector. This study aims to assess the effect of double pass air flow on the performance of flat plate air collectors. The analysis of the performance characteristics of the indirect solar dryer was carried out by CFD simulation with three different smooth, rough and V-grooved surfaces, keeping the lower and lateral collector well insulated and the drying chamber acting as a vertical chimney. The average thermal efficiency of the V-grooved surface, smooth surface, and rough surface is 90%, 78%, and 62% respectively. The total area of the collector is 1.20 × 2.0 = 2.40 m² with the dimension of drying cabinet width, depth, and height 1200 × 650 × 1000 mm respectively. The pressure drop observed at the entrance to the drying chamber is high in the case of a smooth surface, medium in a rough surface and low in a V-grooved plate which will allow sufficient gas pressure to pass through completely. The air mass flow rate is the most important and effective factor during drying. The humidity of the air, as well as air velocity, is also an important factor in improving the drying rate.

Keywords: CFD simulation, V-grooved surface, smooth surface, rough surface, double pass

Article History: Received: 14th February 2020; Revised:11th May 2020; Accepted: 20th June 2020; Available online: 29th June 2020
How to Cite This Article: Desisa D.G, Shekata G.D, (2020) Performance Analysis of Flat-Plate and V-groove Solar Air Heater Through CFD Simulation. *International Journal of Renewable Energy Development*, 9(3), 369-381
https://doi.org/10.14710/ijred.2020.30091

1. Introduction

The flat plate solar collector is a simple device that uses incident solar radiation to obtain solar energy for numerous applications. It converts solar radiation into heat by heating air or water and distributing it for use. The solar air heater can be used for drying agricultural products, seeds and vegetables and some modern applications. Thus, the researchers focused their investigation on improving performance of flat plate solar collector.

Different modifications were suggested and applied to improve the heat transfer coefficient between the absorber plate and the convective medium. Priyam and Chand, (2016) suggest that collector efficiency can be improved by attaching fins to the absorber to extend the heat transfer area. Handoyo *et al*., (2016) conclude from his analysis that application of obstacles to the solar air heater enhances the convection heat transfer between the air and the absorber plate due to turbulences. As a result, efficiency will be improved, but will increase the drop in air pressure.

Kumar *et al.*, (2018) presented the V-type perforated blockage offering better thermal-hydraulic performance compared to other blockage air passages. The air flowing over and under the V- grooved type absorber plate creates turbulence and increases the convective heat transfer coefficient. This leads to improving collector performance.

Several parameters have an influence; the temperature of drying gas is the parameter that mainly influences the drying rate (Burmester & Eggers, 2010). Higher thermal conductivity and convective effects in fluid suspension are important for improving thermal performance with increased weight concentration and flow rate (Sadeghzadeh *et al*., 2019).

The performance of the dryer also depends on heat loss prevention and increasing the absorber area in contact with the air flow. The V-groove enhances the heat transfer between air and absorber by increasing convective surface area (Fudholi *et al.,* 2015; Zulkifle *et al.,* 2018) essential to achieving better efficiency. A V-groove collector is more efficient than a flat plate collector of a similar design, and the efficiency of the collector is very much dependent on the air flow. Zulkifle *et al.*, (2018) reports also show the importance and favourability of V-groove collectors over other designs despite their higher costs; they produce much higher heat transfer coefficients than with flat solar air collectors.

Many researchers have shown interest in Computational fluid dynamics (CFD) due to low time consuming and inexpensive tool for solving problems involving fluid flows. However, CFD simulation can never

* Corresponding author: debelameng@gmail.com ; gadisa3224desa@gmail.com

eliminate the need to build and test prototypes, but it can considerably reduce the number of tests usually required in pure empirical investigations and development. Thus, CFD can be considered as a valuable and general tool for the investigation of the fundamentals of flow systems and their related problems to predict the performance of new process designs before manufacturing or implementation. Olia *et al*., (2019) indicated in their study that numerical studies were the most favourable tool for researchers due to the main reason that can be found on the cost relatively cheaper compared to an experimental study that might need a higher cost for both system setup and material purchase.

To extend the storage life of the agricultural product with the desired quality and reduced volume, the choice of an appropriate drying method is essential. In most rural areas of Ethiopia, Open-air sun drying and outdoor terraces are still common among coffee producers. Among total coffee product of Ethiopia, washed coffee represents 29% while sun-dried coffee represents 71% of the total (Musebe *et al*., 2014; Ali Mohammed, 2014). In the country's economy, around 15 million people depend on coffee production for their livelihood and around 60% of foreign income comes from coffee. However, due to the inappropriate choice of processing, Ethiopian's coffee attains mediocre quality as a result of least priced coffee as compared with the other origins.

The motivation behind this work is to investigate an efficient solar dryer using a CFD simulation analysis to use as an input model for manufacturing. To determine the thermal energy required for drying coffee beans, ensure that the required energy is sufficient or insufficient by analysing the energy flow from a collector inlet to a dryer outlet.

Increasing a temperature enhances the throughput of the batch-process and the efficiency of the process, but the sensitivity of the coffee should be taken into account. The advantages of the V-grooved solar dryer:

- Higher absorber area results in better convective heat transfer movement of the air and lower humidity increases the rate of drying.
- Higher temperatures deter insects and the faster drying rate reduces the risk of spoilage by microorganisms.
- In addition to higher drying rate also gives a higher throughput of product and smaller drying area (approximately one third).

The objective of this work is therefore to analyses heat transfer rate and temperature distribution in an agricultural product dryer by CFD simulation to bring out the effects of solar absorber on the drying rate.

2. Methodology

2.1 Climate Data Collection

The study site location found Latitude 7°41'3.59"N, longitude 36°49'31.79" E., and a moderate climate with hot summer and cold winter. The annual daily average solar radiation reaching the ground in Ethiopia is estimated to be 5.5k Wh/m^2/day which varies from a minimum value of 4.5k Wh/m^2/day in July to a maximum value of 6.5 kWh/m^2/day in February and March (Tesema, 2014)

2.2 Design and CFD simulation analysis

During CFD simulation analysis, the data used were divided into three categories; the first category was general input of metrological data, the second was the specification to manufacturing attributes regarding the collector and its characteristics and the third was the energy characteristic data which contain measured data about inlet temperature and mass flow rate related to the transfer media inside the collector.

Khatibi *et al*., (2019) state modeling is a method to simplify a system better in order to understand and predict its behaviour. CFD modeling and Simulation approach solve real-world problems safely and efficiently. It provides an important method of analysis which is easily verified, communicated and understood (Desisa *et al*., 2016). Across industries and disciplines, simulation and modeling provide valuable solutions by giving clear insights into complex systems:

a) CFD Simulation modeling provides a safe way to test and explore different "what-if" scenarios and provides a risk-free environment.
b) Unlike spreadsheet or solver-based analytics, simulation modeling allows the observation of system behavior over time, at any level of detail, so possible to insight into dynamics.
c) Virtual experiments with simulation models are less expensive and take less time than experiments with real assets so it saves money and time.
d) CFD simulation model can capture many more details than an analytical model, providing increased accuracy and more precise forecasting.
e) CFD Simulation models can be animated in 2D/3D, allowing concepts and ideas to be more easily verified, communicated, understood, and visualized.
f) Uncertainty in operation times and outcome can be easily represented in simulation models, allowing risk quantification.

To begin the iteration, the initial temperature value for glazing (Tc), airflow (T_f), absorber plate (Tp), and base plate (T_b) is estimated. After all, constants where defined, the heat transfer coefficient is calculated as shown in fig.1. The total area of the collector under study was 1.20 m × 2.0 m = 2.40 m^2 with the drying cabinet 1.20 m × 0.65 m × 1.00 m (width × depth × height) and 0.005 m thick glass cover. The insulating material is considered as glass wool shielded by an aluminium foil and wood from the bottom surface of the collector. The distance between the glass cover and the absorber plate is 0.05 m.

The heated convective medium will pass over or through the products to be dried, where the thermal energy is transferred by convection. The convection medium has two advantages along with high drying rate and high moisture removal compared with others; the first consists in transferring the heat for the evaporation of the humidity of the wet product through the convective mode and the second consists in evacuating the evaporated moisture.

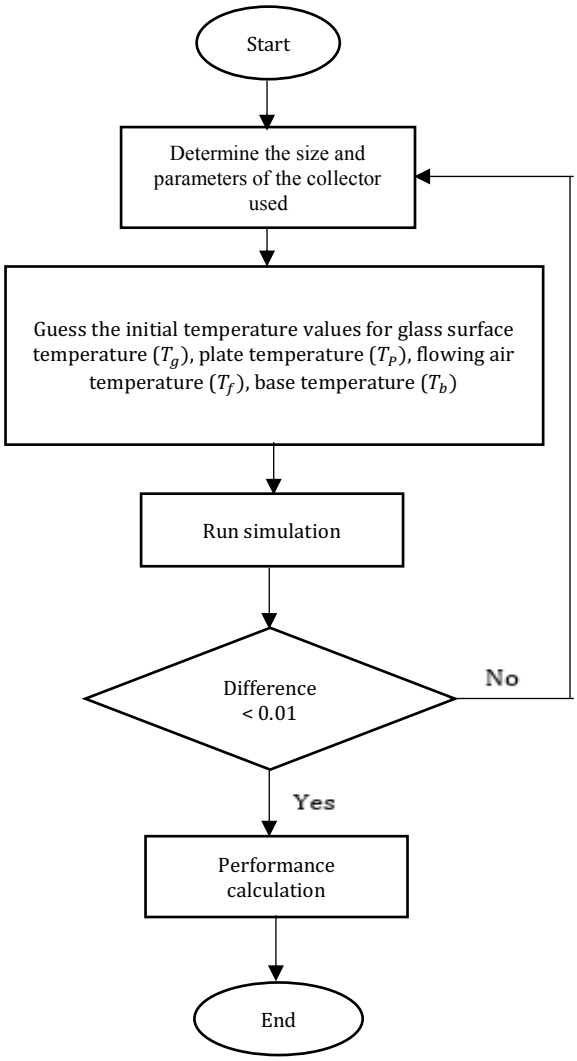

Fig. 1. Simulation flow chart

Table 1
Material properties used for CFD simulation

Types of materials	Thermal conductivity (W/m K)	Density (kg/m³)	Specific heat (kJ/kg K)
Air	0.025	1.069	1007
Aluminium	202.5	2719	871
Glass	1.19	2500	840
Insulation	0.173	700	2310

Source: material property tables

2.3 Double-parallel flow flat plate solar air heater

Ramani *et al.,* (2010) states the flat plate solar collector perform poorly due to high heat loss and low heat convective heat transfer between the absorber plate and air stream. However, flat plate solar collectors are the simplest and widely used for heating and drying applications (Kuhe *et al.*, 2019).

El-Sebaii *et al.,* (2011) indicated that the presence of a V-grooved plate enhances the heat transfer coefficients from the absorber plate to the air flowing in the upper and lower channels due to the formation of turbulence at inside the upper and lower channel.

Alam & Kim, (2017) claimed that the types of air flow patterns are the main factor affecting the performance of the solar air heater. Fig. 2 (a) shows the air flow along the lower and upper faces of the absorber plate. Heat extraction enhances the performance and reduces the overall heat loss to the environment. Manjunath *et al.,* (2018) explained that the presence of V-groove corrugation provides higher flow disturbances leading to a significant enhancement in heat transfer in addition to an increased surface area for convective heat transfer. Fig. 2(b) shows the high velocity flow strike on the leading corrugated surface and gets deflected toward the absorber region forming a recirculation zone.

The performance of a flat-plate solar collector can be described by the useful energy gained from the collector per unit time of a collector area A_c and its difference between the absorbed solar radiation by absorber plate and the thermal loss or the useful energy output of a collector.

The heat gained by the dryer per unit time, Qd is calculated as follow:

$$Q_d = A_C [\alpha\tau I_N - U_L (T_{ai} - T_a)] \quad (1)$$

Where:
- A_C the area of transparent cover (m^2)
- I_N the incident insulation (W/m^2)
- U_L the overall heat loss of the collector (W/ ℃)
- α the solar absorbance
- τ the transmittance
- T_{ai} the incoming air temperature (℃)
- T_a the ambient air temperature (℃)

Since the temperature of the incoming air is equal to the temperature of ambient air, the last term on the right-hand side zero and the rate of energy collection is simply because of the dryer draws the ambient air directly.

$$Q = A_c I \alpha \tau \quad (2)$$

The rate of valuable heat energy gain by flowing air in the course of the duct of a solar air heater can be intended as equation (3) (Tyagi *et al.,* 2012).

If the mass of air leaving the dryer per unit time is m_a, the heat gained by the air Qu is:

$$Q_u = \dot{m} C_{Pa} (Tao - Tai) = h A_c (T_{Pm} - T_{am}) \quad (3)$$

Where:
- C_{pa} is the specific heat capacity of air (kJ/kg K)
- T_{ao} is the out-going air temperature (K)
- h is heat transfer coefficient between the air and absorber plate ($W.m^{-2}K^{-1}$)
- T_{Pm} is mean absorber plate temperature (K)
- T_{am} is mean temperature of air in the air heater duct (K)

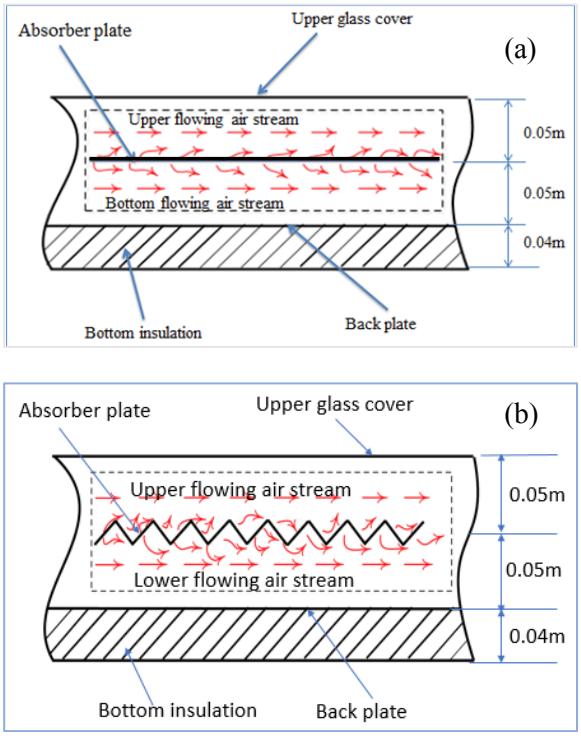

Fig. 2. Inner profile of absorber plate with (a) Double-pass flat plate and (b) Double pass v-grooved plate.

Therefore, a simplified energy equation for the dryer expressed as below; $Q_d = Q_u$

$$Q_u = \dot{m}_a C_{Pa}(T_{ao} - T_{ai}) \quad (4)$$

and the required surface area of the transparent cover which determines the size and dimensions of the dryer is obtained from:

$$A_c = \frac{\dot{m}_a * C_{pa}(T_{po} - T_{ai})}{(\tau\alpha)\, I_N \eta_c} \quad (5)$$

Where,

- C_{pa} is the specific heat capacity of air (kJ/kg K)
- T_{po} is outgoing air temperature from the absorber plate (K)
- T_{ai} the incoming air temperature (K)
- η_c is collector efficiency
- $(\tau\alpha)$ is transmittance-absorbent product of glass cover

The total energy required for drying a given quantity of coffee beans can be estimated using the basic energy balance equation for the evaporation of water.

$$M_W h_{fg} = \dot{m}_a C_{Pa}(T_{ao} - T_{ai}) \quad (6)$$

Where:

- h_{fg} is the specific heat of vaporization, (kJ/kg)
- M_W is the mass of evaporated water, (kg /s)

The mass of water is estimated from the initial moisture content M_i and the final desired moisture content M_f. The total quantity of moisture to be removed from the coffee beans to bring it to the desired moisture from the initial moisture content is used to determine the total mass flow of air required for drying. The quantity of moisture to be removed (M_w) depends on the coffee parchment and can be found from the following relationship:

$$M_W = m_{cb} \frac{M_i - M_f}{100 - M_f} \quad (7)$$

Where:

- M_W is the water removed per kg of the airflow, (kg)
- m_{cb} is the mass of coffee beans, (kg)
- M_i is the initial moisture content of coffee (% of dry)
- M_f is the final moisture content of coffee (% of dry)

During drying, water from the surface of the substance evaporates and water in the inner part migrates to the surface to get evaporated. The ease of this migration depends on the porosity of the substance and the surface area available.

Abuşka & Şevik,(2017) experimentally investigated the V-grooved surface has better efficiency than a flat solar air collector even if the flat plate solar air collector can be considered a suitable choice for hot air applications. To drive up the thermal efficiency of solar collector increasing the mass flow rate is a remarkable coincidence which is provided in the equation (8) (Fudholi *et al.*, 2015).

$$\eta = \frac{Q_u}{A_f \bullet I} = \frac{\dot{m}C(T_o - T_i)}{A_f \bullet I} \quad (8)$$

Where:

- C is specific heat of the fluid, $(J.kg^{-1}.°C^{-1})$
- A_f is the area of the collector (m^2)
- I is the solar radiation incident on the collector (W/m^2)
- T_o is outgoing air temperature, (°C)
- T_i is incoming air temperature, (°C)

2.2.1 Energy Balance for the Drying Process

Finding the optimum value of geometric parameters involves the simultaneous deliberation of the enhancement of thermal performance and the minimization of friction losses (Alam *et al.* 2014).

Heat and mass balance of the first tray calculated as follow:

$$(\dot{m}_a C_P)_a (T_2 - T_1) = M_{W1} h_{fg} \quad (9)$$

Where:

- $\dot{m}_a$ is dry air mass flowrate, (kg/s)
- T_1 is the temperature of the air entering the first tray, (K)
- T_2 is the temperature of the air leaving the first tray, (K)

The temperature of the air stream outgoing from the first tray of the drying chamber at the ambient conditions at the time $(t + \Delta\tau)$ gains energy from the incident radiant energy on the collector plate and black wall of the drying chamber in the first tray (Fig 3) is determined from:

$$T_2 = T_1 - \frac{M_{w1}\, h_{fg}}{(\dot{m}C_P)_a} \Delta\tau \quad (10)$$

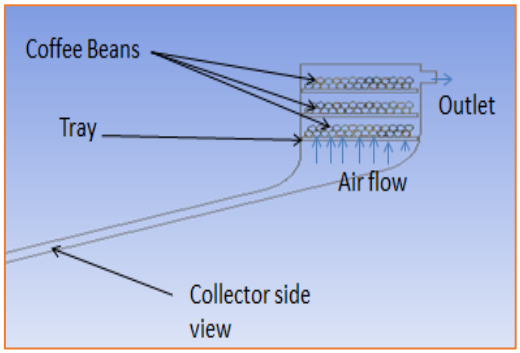

Fig. 3. A batch of grain(coffee) on the tray for drying during operation from the first tray to the third tray and airflow entering from a bottom.

Heat and mass balance on the second tray are calculated as follow:

$$(\dot{m}_a C_P)_a(T_{2d} - T_{1d}) = M_{W2} h_{fg} \quad (11)$$

Where:

- T_{1d} is the temperature of the air entering the second tray (K)
- T_{2d} is the temperature of the air leaving the second tray (K)

The temperature of the air stream outgoing from the second tray of the drying chamber at the ambient conditions at the time ($t + \Delta\tau$) gains energy from the incident radiant energy on the collector plate and black wall of the drying chamber in the second tray is calculated from:

$$T_{2d} = T_{1d} - \frac{M_{w1}\, h_{fg}}{(\dot{m} C_P)_a} \Delta\tau \quad (12)$$

2.2.2 Heat Loss Coefficient of Flat Plate Collector

It is useful to develop the concept of an overall loss coefficient for a solar collector.

$$\dot{Q} = U_L A_C (T_{Pm} - T_a) \quad (13)$$

Where:

- U_L is the overall heat loss coefficient, ($W \cdot m^{-2} \cdot K^{-1}$)
- A_c is the area of the collector (m^2)
- T_{pm} is the mean temperature of the absorber plate (K)
- T_a is the temperature of the air (K)

2.2.3 Average drying rate

The drying rate is the amount of water removed per unit time per unit mass of dry matter to achieve a desired state of dryness. From the three main regions of moisture sorption isotherm; strongly bound water, less firmly bound water, excess/free water regions, the average drying rate, m_{dr}, can be determined from equation (14) .

$$m_{dr} = \frac{M_w}{t_d} \quad (14)$$

Where:

- Drying time (t_d) $= \frac{Mw}{\dot{m}_a (w_f - w_i)}$
- m_{dr} is drying rate
- M_w is the water removed per kg of the airflow (kg)
- W_i is initial humidity ratio per kg of dry air
- W_f is final humidity ratio per kg of dry air

The mass of air needed for drying calculated using the equation given as follows:

$$\dot{m}_a = \frac{m_{dr}}{W_f - W_i} \quad (15)$$

Gautz *et al.* (2008) suggest that for 70% ambient relative humidity, coffee beans will gradually equilibrate to about 12% moisture. Thus, the green coffee bean is generally dried to 12% and bought and sold at this moisture percentage. If the bean dries below 9% moisture, it will shrink enough to distort, giving the appearance of poor-quality coffee. The humidity of the dried coffee should be around 11% (Burmester & Eggers, 2010).

The drying rate can be affected by different parameters; one of the parameters that affects the drying rate is the mass flow rate of hot air. For the sample taken, 50 kg of parchment coffee beans at 46 ℃ dried in 5 – 8 days in the mass flow rate of 0.01 kg/s, but the same amount of sample dried in 1 – 2 days at 0.06 kg/s air mass flow rate in V-grooved absorber plate. In the case of another absorber, smooth and rough plate, this drying rate decreases for the same sample and the same flow rate to reach a required level of moisture content due to a decrease in temperature.

3. Description of computational Model

The absorber plays a greater role in maximizing the ability of collectors to absorb solar intensity. A large convective surface area introduces a greater rate of heat transfer and air movement. The model considered for the computational domain of the rectangular flat plate having smooth, rough, and V-grooved surface directly connected to the dryer chamber that helps as a chimney. The dimension of the collector length, width, and height are 2000 mm, 1200 mm, 100 mm respectively with a total area of 2.40 m^2. The investigation has been carried out for different geometries of the absorber plate of solar collector, i.e. smooth flat plate, rough flat plate, and V-grooved corrugated surface in all double pass air streams have been adopted. To discretize the flow domain, the unstructured two-dimensional mesh was created for all simulation cases.

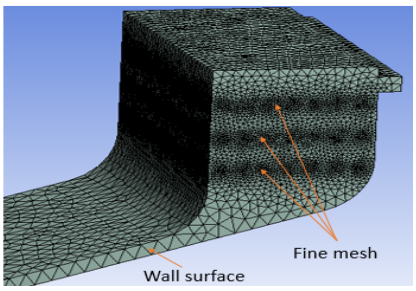

Fig. 4. Meshing a model

The numerical simulations preferred was finite volume method for all geometries considered in this present work.

3.1 Boundary condition and governing equations

Simulation results were generated taking an optimal number of mesh elements by selecting finite volume method (FVM) for the discretization. The upper surface of the absorber plate of the domain was exposed to a uniform heat flux of 600, 700, 900 W/m^2. The side and bottom walls of the collector were insulated (adiabatic). The inlet and outlet flow domains were set as mass flow inlet (mass flux of air, kg/m^2) and pressure outlet (standard ambient pressure taken as reference), respectively. The fluid material is air.

The flow is two-dimensional, incompressible, in steady state, density-based and absolute solver type. The treatment of the walls of the k-ε turbulence model with two equations of the viscous model was preferred throughout the numerical analysis. After having realized boundary conditions on the flow domain, the following governing equations i.e. continuity, x and y momentum, energy, and turbulence dissipation rate ε equations were solved for the two-dimensional numerical analysis. A steady state numerical analysis using the SIMPLE algorithm (semi-implicit method for pressure linked equations) selects to solve the velocity and pressure field for the discretized computational flow domain. Convergence criteria have been considered of order 10^{-3} for energy equation and 10^{-5}order for the velocity component and the momentum equation.

Continuity equation

$$\frac{\partial \rho}{\partial t} + \nabla.(\rho V) = 0 \tag{16}$$

Momentum equations

$$\frac{\partial(\rho u)}{\partial t} + \nabla.(\rho u V) = \frac{\partial p}{\partial x} + \mu\nabla(\nabla.u) + \rho g_x \tag{17a}$$

$$\frac{\partial(\rho v)}{\partial t} + \nabla.(\rho v V) = \frac{\partial p}{\partial x} + \mu\nabla(\nabla.v) + \rho g_y \tag{17b}$$

Energy equation

$$\rho C_P\left(\frac{dT}{dt} + \nabla(TV)\right) = \nabla(\nabla.kT) \tag{18}$$

Where:

- ρ is density of air, kg/m^3
- V is fluid Volume, m^3
- u, v is flow velocity in x and y direction, respectively, m/s
- T is temperature, K
- p is fluid density, kg/m^3
- k is thermal conductivity, W · m^{-1} · K^{-1}
- ρg denotes force density
- ∇ denotes the gradient with respect to space

Reynolds Number

$$\mathrm{R_e} = \frac{\text{Inertia force}}{\text{viscous force}} = \frac{\rho\, \mathrm{u}\, D}{\mu} \tag{19}$$

Dean Number,

$$D_n = R_e\sqrt{\frac{D_H}{R_C}} \tag{20}$$

Where:

- ρ is the density of the fluid, kg/m^3
- μ is dynamic viscosity of air, N · s · m^{-2}
- D is diameter of the duct, mm
- u is the flow speed, m/s
- D_H hydraulic diameter, mm
- R_C is curvature radius of the path of the curved channel of SAH, mm

Where $D_H = \frac{H}{2}$ (half of the height of the duct passage of SAH). Reynolds number (R_e) and dean number D_n) are the important dimensionless parameters to differentiate among laminar and turbulent flow in straight and curved flow duct passage respectively (Mahboub *et al.,* 2016; Nivedita *et al.,* 2017; Singh & Singh, 2018). However, in this present simulation Reynolds number (Re) and Dean number (D_n) are in the range of 2209–6058 and 180–494, respectively which comes under turbulent range (Mahboub *et al.*, 2016; Nivedita *et al.,* 2017; Singh & Singh, 2018), hence turbulent flow model has been considered during the entire simulation run.

4. Result and Discussion

Factors affecting the performance effectiveness of solar dryers include air temperature, air velocity, and porosity of product, layer thickness, and moisture content of the product. Other factors are humidity of the surrounding air, method of drying, moisture diffusivity, and drying kiln structure (Bolaji & Olalusi, 2008; Şevik, 2013).

In corrugated duct due to the formation of backflow and high velocity in the gap between obstacle and absorber plate flow becomes more turbulent and enhanced the convection heat transfer, in turn, improve efficiency but increase the air pressure drop (Handoyo et al., 2016).

4.1. Effect of absorber plate on output temperature

In solar collectors, the heat transfer capacity determined by mass flow rate, which induces higher velocities via the perforations and more heat transfer from the plate to the air. Shukla *et al*., (2018) state in their report a moving air in contact with absorber surface for more time at a lower flow rate.

Drying rates are determined by the rate at which heat energy can be transferred to the product to provide the latent heat. Yousef & Adam, (2017) also reported increasing mass flow rate the thermal efficiency of the system increases but outlet temperature decreases, alluding double-flow mode which is more efficient than single flow due to the increased heat removal for two channels. The excremental study done by Pakhare & Salve, (2011) in chilly drying reports increases the mass flow rate, the exit temperature of collector decreases, and suggests 0.01 kg/s is the maximum flow rate to be kept for drying. The temperature drop is a significant indicator of the mass flowrate effect on collector efficiency *(*Zulkifle *et al*., 2018).

In this analysis, flow rate lower than 0.01 kg/s was not taken into account at the low mass flow rate, High temperature was observed, but by increasing mass flow rate, the temperature decreases. With increasing in mass flow rate (kg/s), the amount of volume of air passing over the absorber is thick, so that the molecule of the moving air in contact with convective surface area will be less. On the other hand, as hot air passing through the porous of agricultural product, the water vapour from the grain perform heat exchanger with hot air through convection. Due to this, the outlet temperature is decreasing vertically upward through the compartment.

Employing the V-grooved absorber maximize contact surface area to improve the heat transfer from the absorber plate to the fluid flow. Figure 5 shows as the mass flow rate increases from 0.01 kg/s to 0.06 kg/s, the output temperature declines for different absorber plates. The V-grooved absorber attains 52 ºC outlet temperature at mass flow rate 0.01 kg/s while smooth and rough absorber surface attains 47ºC and 46ºC outlet temperature, respectively.

For a range of mass flow rates understudy, as the mass flow rate rises from 0.01 kg/s to 0.06 kg/s non-leaner falling change in temperature was observed. At 0.06 kg/s the V-grooved absorber falls from 52 ℃ to 46 ℃ while smooth and rough surface absorber falls from 47 ℃ and 46 ℃ to 41℃ and 40℃ respectively under the same boundary condition.

4.2. Effect of absorber plate on hot air velocity

Since the density of a heated air decreases the ambient air with a higher density replace the hot air where the drying chamber act as a vertical chimney. As a result, a buoyancy force acts to produce a draft that sucks air from the collector even if the pressure drops due to friction, ninety-degree bend (pressure head), and trays also exists. Very low air velocities would have resulted in very high drying air temperatures while high velocities would result to low air temperatures.

Velocity is the function of the flow rate of the fluid, the area, and density of the fluid. The increase in mass flow rate will subsequently increase the flow velocity which in turn will increase the overall heat transfer coefficient. On the other hand, sufficient velocity of the fluid is necessary to create sufficient turbulence which maintains suspension. The greater the volume of fluid in contact with the surface of the convective area, the greater the heat transfer. The higher the velocity of the fluid, the higher the turbulence and more efficient in heat transfer.

Fig. 6 shows that air velocity ranges from 0.18 m/s to 1.40 m/s for V-grooved absorber plate and 0.1m/s to 0.40 m/s in smooth and rough flat plate. This result is in concurrence with the result of the most researcher (Koua *et al.*, 2009; Afriyie et al., 2009; Gatea, 2011; Aziz *et al.*, 2016) on the rage of air velocities from 0.22 m/s to 2 m/s. But, (Şevik, 2013) reported that air velocities above 0.42 m/s do not influence drying rate.

Mass flow rate is the measure of the mass of fluid passing over an absorber area in the system per unit time. At low mass flow rate 0.01 kg/s, the V-grooved absorber attains 0.18 m/s velocity, but it increases with mass flow rate and at 0.06 kg/s the velocity reaches 1.4 m/s but, during the smooth and rough surface, air velocity attain 0.06 m/s at 0.01 kg/s mass flow rate, increasing with mass flow rate it reaches 0.4 m/s at 0.06 kg/s as shown in Fig.6.

In the solar dryer, outlet temperature and air velocity are inversely proportional to mass flow rate, therefore, searching for the optimum value of drying rate concerning mass flow rate is necessary.

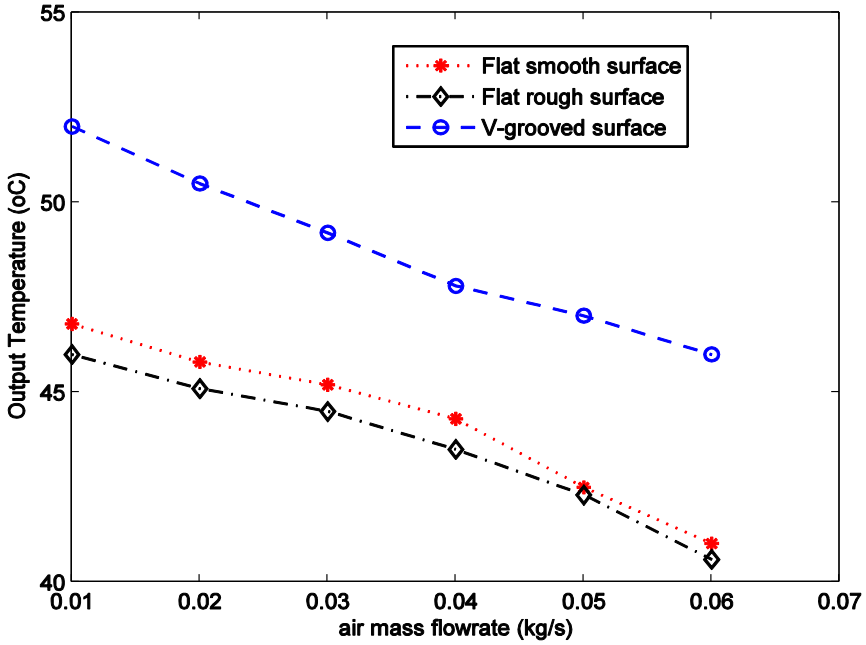

Fig. 5. Effect of mass flow rate on outlet temperature

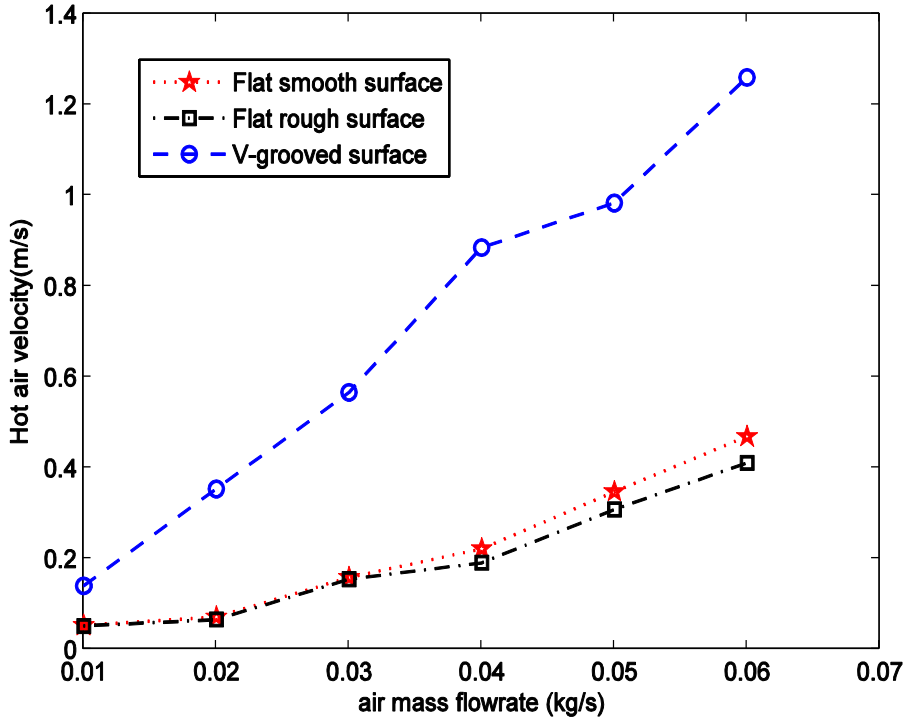

Fig.6. The effect of air mass flow rate on hot air velocity

4.3. Effect of absorber plate on thermal efficiency

For a fixed mass of coffee where the same range of air mass flow rates was supplied, different collector efficiency was observed due to the absorber effect. Absorber surface geometry has a great role in increasing the convective heat transfer rate by increasing the effective area of the heat exchanger and receiving solar radiation.

The area of absorber significantly affects the convectional heat transfer to the flowing fluid. Fig. 7 shows that when the mass flow rate increases from 0.01 kg/s to 0.06 kg/s the thermal efficiency increases. Improved thermal efficiency can be achievable by using the small size of V-groove absorber and reducing collector heat loss.

The thermal efficiency demonstrates that the fraction of heat becomes useful among the heat gain (application of drying). The thermal efficiency of the system was 10% at 0.01 kg/s, then increased with increase in mass flow rate to 0.06 kg/s attaining 94.6% during V-grooved absorber plate, 76% during smooth absorber plate and 60% during rough absorber plate. The percentage increase during the V-grooved absorber plate is 14% comparing with a smooth surface and 30% compared with the rough surface plate. This is due to the improvement in internal convective heat exchangers at a constant heat loss when the air flow increases. There is a fact that at a lower mass flow rate, the amount of energy spent to overcome the friction loss is lower. The friction loss increases sharply as the mass flow rate increases for which the energy required to overcome this friction loss is high. In this analysis, the mass flow rate lower than 0.01 kg/s and higher than 0.06 kg/s was not taken into account, it is necessary to find the optimum flow and to maintain the constant.

The thermal efficiency of the dryer also influenced by relative humidity in the air, moisture content of products to be dried, the porosity of the product, and their amounts for a batch dryer.

When comparing a CFD simulation obtained in this work with the experimental result obtained by Karim & Hawlader, (2006) the result shows a much difference at the start 0.01 kg/s mass flow rate due to the heating before a test conducted in the case of experiment work as stated under test procedure. At mass flow rate 0.06 kg/s, the simulation result shows greater efficiency in both flat plate and V-grooved mode of air collector comparing with the experimental result obtained.

4.4. Effect of mass flow rate on pressure drop

Pressure drop is determined by measuring the pressure of fluid entering into the studying area and leaving it. It is the amount of line pressure that is lost permanently when the gas passes through an area in the gas line. Pressure drop can be presented as the ratio of the friction factors for straight and curved pipe under the same conditions based on the actual centreline length of the curvature.

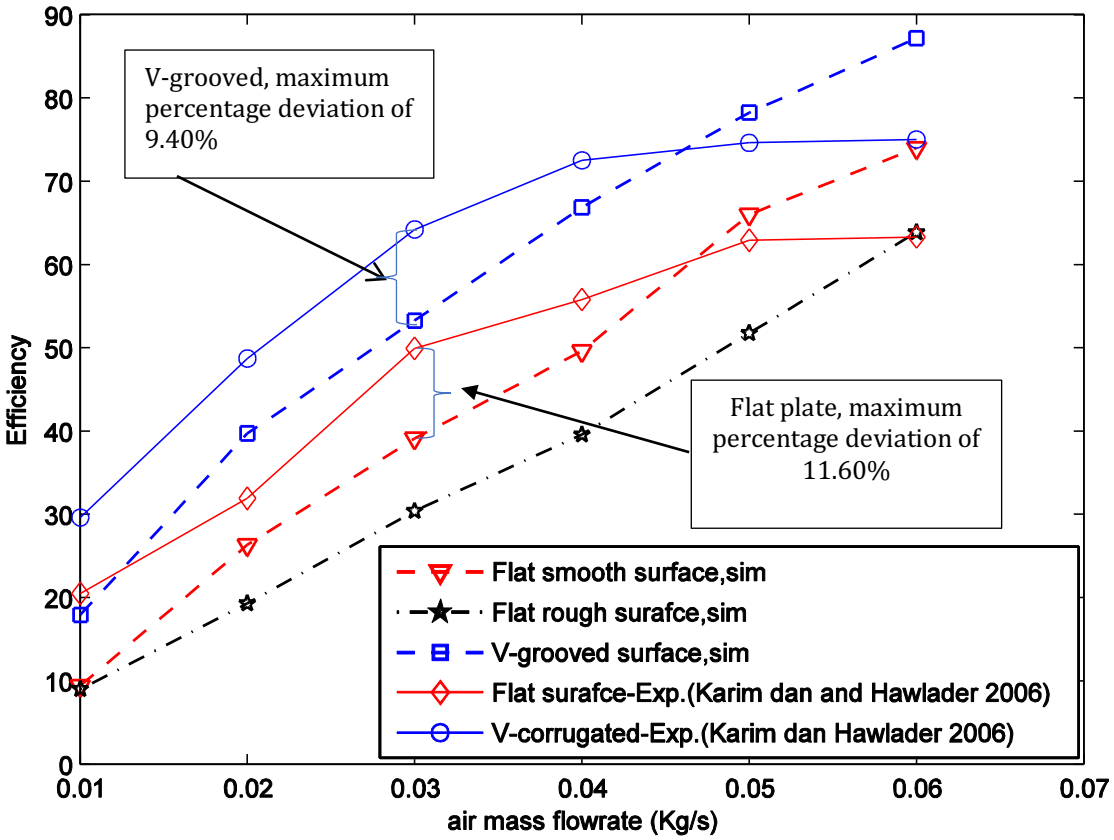

Fig. 7. Effect of mass flow rate on thermal efficiency for different absorber plate

Consideration of pressure drop may be critical in a certain situation in elevation of heat transfer medium and benefit gained from the higher heat transfer coefficient lost because of the higher pressure drop across the flow line in constant area case. Every instrument with fitting in line induces pressure drop whereas the pipe walls generate some friction causes a small amount of pressure drop. If the high-pressure drop is observed at the inlet of the drying chamber, there will not be enough gas pressure to pass through all the compartment of the process at full-scale flows.

Fig. 8 shows the relation between the pressure drop and the mass flow rate in the solar dryer while V-grooved, rough, and smooth absorber plates were the three comparative absorber surfaces. The pressure drops increase as the mass flow rate increase due to the increased velocity of air flow along with increase in mass flow rate. The presence of V-groove increases the velocity of the fluid due to the collision between molecules increases resulting in greater loss of kinetic energy, in turn, the high pressure drops observed. On the other hand, increasing the gas temperature increases its viscosity, as a result, pressure drop also increases. In reality, the fluid flow between two points cannot be achieved without a loss of fluid energy due to friction, fitting in a line and changes in momentum.

In laminar flow conditions, the pressure drop is proportional to the volumetric flow rate, but in turbulent flow, pressure drop increases as the square of the volumetric flow rate. Due to the presence of a V-groove surface, a turbulent flow condition is formed which increases the pressure drop with an increased mass flow rate of a gas. The power required to overcome the pressure drop formed across the flat and V-grooved absorber plate is negligible as many pieces of literature agree and reported.

The result of pressure drops almost agree with the experimental result obtained by El-Sebaii et al., 2011 with a maximum percentage deviation of 7.7% and 6.1% in v-grooved and flat plate absorber respectively.

4.5 Effect of RH on equilibrium moisture content

The equilibrium moisture content (EMC) is the moisture content at which the material neither gains nor loses moisture. The value of the EMC depends on the material and the relative humidity and temperature of the air with which it is in contact. (Grain Crop Drying, Handling, and Storage, FAO.2011) reports for most cereals EMC vary slightly with temperature and drops by approximately 0.5 percent for every 10 °C temperature rise at the same percentage relative humidity of the air.

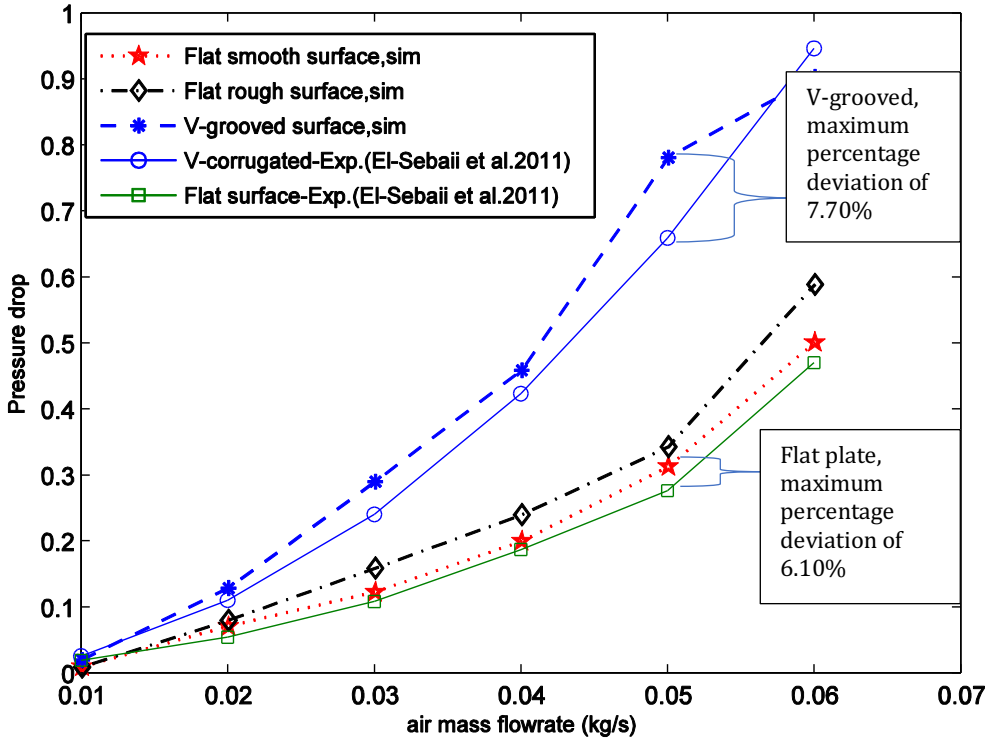

Fig. 8. Effect of air mass flow rate on pressure drop

The relative humidity is the ratio (in percentage) of the amount of moisture in the air to the maximum amount it can hold at a given temperature, while the dew point temperature is the point at which relative humidity reaches 100%; hence, the saturation temperature. Because the warm air can hold more water vapor than the cold air, the relative humidity changes with temperature. All agricultural product exerts a vapor pressure at a certain temperature and moisture and all porous food (product) materials adsorb or desorb water molecules to attain equilibrium moisture content when in contact with moist. The equilibrium moisture content depends strongly on the relative humidity of the surrounding air and rather weakly on the air temperature of the drying. At low relative humidity equilibrium moisture content, the EMC was low, but RH increases proportionally, EMC also increases, as shown in Figure 9 below by sorption isotherm curve best fit to R^2 equal to 0.9991.

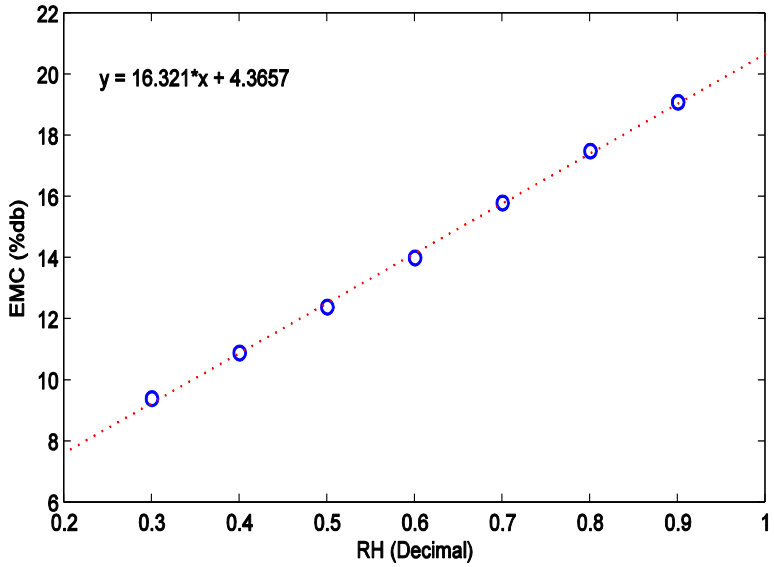

Fig.9. Variation of equilibrium moisture content with RH

5. CFD Simulation Analysis

In the flat plate dryer, due to high pressure from the behind, the heated air is rushing to the outlet vent forming low pressure region around the top inside of the dryer chamber. This affects the uniformity of the dried product, especially in batch drying products. In the double pass absorber, heated air moves parallel on the top and bottom of the absorber till it reaches to the bottom region of the dryer chamber. The upward movements through the chamber are not uniform due to mixing up of two parallel moving air even if this has an advantage in retaining heated air in the product.

In Steady flow, each particle passing through the second point behaves the same as the previous fluid particle initially crossed that point. The major characteristic of the streamline flow of a fluid depends on velocity. Fig. 10(a) shows the behavior of fluid flow inside the drying compartments passed over a smooth flat plate indicating laminar flow. Fig. 10(b) shows the behavior of fluid flow inside the compartments passed over a V-groove plate indicating turbulent flow. Fig. 10 (a & b) shows the property of convection heat transfer is not depend on an intrinsic property of material rather heat flux at the surface and temperature potential difference.

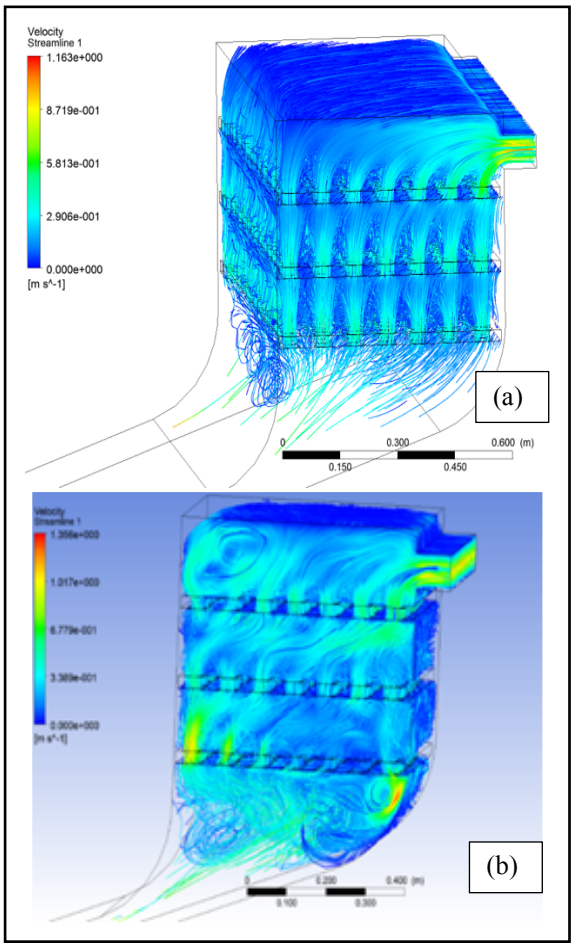

Fig. 10. Velocity streamlines: (a) Flat surface and (b) V-grooved surface

The fluid velocity vector indicates the magnitude and the direction of a flow where a velocity head is a pressure that is needed to increase the speed at which a fluid flow. Due to an increase in the velocity head, there is a drop in pressure head, causing a partial vacuum in the suction chamber (dryer chamber). Fig. 11(a) indicates the velocity profile of hot air passed over a smooth absorber surface generating velocity vector ranging from 0.00 to 1.128 m/s. Fig. 11(b) indicates a velocity vector generated after hot air passed over the V-grooved surface range from 0 to 1.356 m/s.

The pressure drop can be expressed as the sum of two factors: 1) due to friction in the straight pipe which depends mainly on the Reynolds number (surface roughness); 2) due to change of direction, expressed in terms of a bend loss coefficient, mainly depends on the curvature ratio and the bend angle. The fluid in the center of the pipe moves toward the outer side (resistance to change flow direction) and returns along the wall towards the inner side.

Fig. 12 illustrates the pressure gradient near the outer wall in the bend and raises the pressure loss. A low flow velocity results in a lower pressure drop and a high flow velocity result in a larger pressure drop across a section of pipe or a valve or elbow. Due to a 90° bend, a high head loss (energy loss) has been observed. The formation of flow separation, secondary flow and swirling of the flow are contributes to a higher mixing and by this higher loss. Even in bends, in addition to the friction loss, the loss due to the viscous interaction between fluid layers is more.

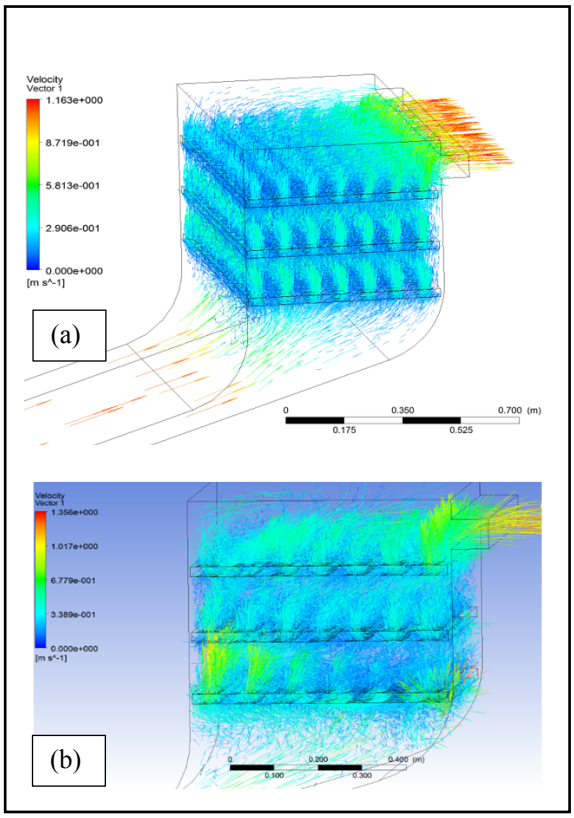

Fig. 11. Velocity vector: (a) flat surface and (b) v-grooved surface

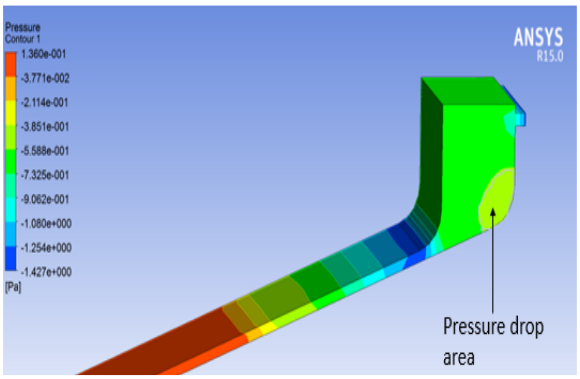

Fig.12. Pressure drop area

This flow separation is due to a local adverse pressure gradient and within a short downstream distance, the flow is re-attached to the wall. At the same time, the primary flow cross-section increases. As the swirl flow outer layers reach the intrados side, they mix with the accelerated flow passing near to the inner wall side and shifted to the middle region.

6. Conclusion

From this numerical analysis, heat absorber has an invaluable role in enhancing the collector thermal efficiency, moisture to be removed and reducing the drying rate. The solar collector is affected by properties of dryer material, while humidity and mass flow rate of air is strongly influencing the collector efficiency. The CFD simulation has a great role in predicting the effect of different parameters on the solar collector that can be easily verified, communicated and understood so that answer the questions what-if" scenarios and provides a risk-free environment.

- Among the three-absorber plate understudy, the collectors with V-grooved (corrugated) absorber plate read high preferable performance in thermal efficiency, output temperature, airspeed and high pressure drop.
- The maximum outlet air temperature found 350 ℃ during the V-grooved plate and 333 ℃ during normal rectangular plates for the same air flow rate.
- For mass flow rate ranges from 0.01 kg/s to 0.06 kg/s, air velocity ranges from 0.18 m/s to 1.4 m/s during v-grooved plate and 0.1m/s to 0.40 m/s speed observed during normal flat plate absorber.
- The double pass absorber leading alongside stream flow is preferable to use both the upper and the lower surface of the absorber plate whereas the V-grooved surface gets deflected toward the absorber region forming recirculation zone.
- The larger the convective surface area, the greater the rate of heat transfer and the faster the rate of air movement.

For further investigation, validating the quantitative analysis with qualitative data may recommendable taking into account the results obtained in this study.

Conflict of interest

The authors declared that there is no conflict of interest.

References:

Abuşka, M., & Şevik, S. (2017). Energy, exergy, economic and environmental (4E) analyses of flat-plate and V-groove solar air collectors based on aluminum and copper. *Solar Energy*, *158*(August), 259–277. https://doi.org/10.1016/j.solener.2017.09.045

Afriyie, J. K., Nazha, M. A. A., Rajakaruna, H., & Forson, F. K. (2009). Experimental investigations of a chimney-dependent solar crop dryer. *Renewable Energy*, *34*(1), 217–222. https://doi.org/10.1016/j.renene.2008.04.010

Alam, T., & Kim, M. H. (2017). Performance improvement of double-pass solar air heater – A state of art of review. *Renewable and Sustainable Energy Reviews*, *79*(May), 779–793. https://doi.org/10.1016/j.rser.2017.05.087

Alam, T., Saini, R. P., & Saini, J. S. (2014). Experimental investigation on heat transfer enhancement due to V-shaped perforated blocks in a rectangular duct of solar air heater. *Energy Conversion and Management*, *81*, 374–383. https://doi.org/10.1016/j.enconman.2014.02.044

Ali Mohammed, B. T. (2014). Impact of Sun Drying Methods and Layer Thickness on the Quality of Highland Arabica Coffee Varieties at Limmu, Southwestern Ethiopia. *Journal of Horticulture*, *01*(03), 547–554. https://doi.org/10.4172/2376-0354.1000117

Aziz, A., Ur, S., & Rehman, S. U. (2016). *Exergy Analysis of Solar Cabinet Dryer and Evaluate the Performance Enhancement of Solar Cabinet Dryer by Addition of Solar Reflectors*. *6*(4).

Bolaji, B. O., & Olalusi, A. P. (2008). Performance Evaluation of a Mixed-Mode Solar Dryer. *AU Journal of Technology*, *11*(4), 225–231. http://www.journal.au.edu/au_techno/2008/apr08/journal114_article05.pdf

Burmester, K., & Eggers, R. (2010). Heat and mass transfer during the coffee drying process. *Journal of Food Engineering*, *99*(4), 430–436. https://doi.org/10.1016/j.jfoodeng.2009.12.021

Desisa, D. G., Ramayya, V., & Tiba, G. S. (2016). *Development Research Product Development Through Cfd Simulation and Experimental Testing of a 200 Liter Biomass Fired Institutional Cook Stove*.

El-Sebaii, A. A., Aboul-Enein, S., Ramadan, M. R. I., Shalaby, S. M., & Moharram, B. M. (2011). Investigation of thermal performance of-double pass-flat and v-corrugated plate solar air heaters. *Energy*, *36*(2), 1076–1086. https://doi.org/10.1016/j.energy.2010.11.042

Fudholi, A., Sopian, K., Bakhtyar, B., Gabbasa, M., Othman, M. Y., & Ruslan, M. H. (2015). Review of solar drying systems with air based solar collectors in Malaysia. *Renewable and Sustainable Energy Reviews*, *51*, 1191–1204. https://doi.org/10.1016/j.rser.2015.07.026

Gatea, A. A. (2011). Design and construction of a solar drying system, a cylindrical section and analysis of the performance of the thermal drying system. *African Journal of Agricultural Research*, *6*(2), 343–351. https://doi.org/10.5897/AJAR10.347

Gautz, L. D., Smith, V. E., & Bittenbender, H. C. (2008).

Measuring Coffee Bean Moisture Content. *Cooperative Extension Service*, *June*, 2–4.

Grain crop drying , handling and storage. (n.d.).

Handoyo, E. A., Ichsani, D., Prabowo, & Sutardi. (2016). Numerical studies on the effect of delta-shaped obstacles' spacing on the heat transfer and pressure drop in v-corrugated channel of solar air heater. *Solar Energy*, *131*, 47–60. https://doi.org/10.1016/j.solener.2016.02.031

Karim, M. A., & Hawlader, M. N. A. (2006). Performance investigation of flat plate, v-corrugated and finned air collectors. *Energy*, *31*(4), 452–470. https://doi.org/10.1016/j.energy.2005.03.007

Khatibi, A., Razi Astaraei, F., & Ahmadi, M. H. (2019). Generation and combination of the solar cells: A current model review. *Energy Science and Engineering*, *7*(2), 305–322. https://doi.org/10.1002/ese3.292

Koua, K. B., Fassinou, W. F., Gbaha, P., & Toure, S. (2009). Mathematical modelling of the thin layer solar drying of banana, mango and cassava. *Energy*, *34*(10), 1594–1602. https://doi.org/10.1016/j.energy.2009.07.005

Kuhe, A., Ibrahim, J. S., Tuleun, L. T., & Akanji, S. A. (2019). Effect of air mass flow rate on the performance of a mixed-mode active solar crop dryer with a transpired air heater. *International Journal of Ambient Energy*, *0750*. https://doi.org/10.1080/01430750.2019.1653970

Kumar, R., Kumar, A., Chauhan, R., & Maithani, R. (2018). Comparative study of effect of various blockage arrangements on thermal hydraulic performance in a roughened air passage. *Renewable and Sustainable Energy Reviews*, *81*(August 2017), 447–463. https://doi.org/10.1016/j.rser.2017.08.023

Mahboub, C., Moummi, N., Brima, A., & Moummi, A. (2016). Experimental study of new solar air heater design. *International Journal of Green Energy*, *13*(5), 521–529. https://doi.org/10.1080/15435075.2014.968922

Manjunath, M. S., Karanth, K. V., & Sharma, N. Y. (2018). Numerical investigation on heat transfer enhancement of solar air heater using sinusoidal corrugations on absorber plate. *International Journal of Mechanical Sciences*, *138–139*, 219–228. https://doi.org/10.1016/j.ijmecsci.2018.01.037

Musebe, R., Agwanda, C., & Mekonen, M. (2014). *Primary coffee processing in Ethiopia : patterns , constrains and determinants Primary coffee processing in Ethiopia : patterns , constraints and determinants*. *January 2007*.

Nivedita, N., Ligrani, P., & Papautsky, I. (2017). Dean Flow Dynamics in Low-Aspect Ratio Spiral Microchannels. *Scientific Reports*, *7*(March), 1–10. https://doi.org/10.1038/srep44072

Olia, H., Torabi, M., Bahiraei, M., Ahmadi, M. H., Goodarzi, M., & Safaei, M. R. (2019). Application of nanofluids in thermal performance enhancement of parabolic trough solar collector: State-of-the-art. *Applied Sciences (Switzerland)*, *9*(3). https://doi.org/10.3390/app9030463

Pakhare, V. V, & Salve, S. P. (2011). Design and Development of Solar Dryer Cabinet with Thermal Energy Storage for Drying Chilies. *International Journal of Current Engineering and Technology*, *5*(5), 358–362. https://doi.org/10.14741/ijcet/22774106/spl.5.6.2016.67

Priyam, A., & Chand, P. (2016). Thermal and thermohydraulic performance of wavy finned absorber solar air heater. *Solar Energy*, *130*, 250–259. https://doi.org/10.1016/j.solener.2016.02.030

Ramani, B. M., Gupta, A., & Kumar, R. (2010). Performance of a double pass solar air collector. *Solar Energy*, *84*(11), 1929–1937. https://doi.org/10.1016/j.solener.2010.07.007

Sadeghzadeh, M., Ahmadi, M. H., Kahani, M., Sakhaeinia, H., Chaji, H., & Chen, L. (2019). Smart modeling by using artificial intelligent techniques on thermal performance of flat-plate solar collector using nanofluid. *Energy Science and Engineering*, *7*(5), 1649–1658. https://doi.org/10.1002/ese3.381

Şevik, S. (2013). Design, experimental investigation and analysis of a solar drying system. *Energy Conversion and Management*, *68*, 227–234. https://doi.org/10.1016/j.enconman.2013.01.013

Shukla, A. P., Kushwaha, R., Gupta, B., & Bisen, A. (2018). Performance Analysis of Solar Air Heater using CFD Simulation. *International Journal of Thermal Technologies*, *8*(01), 1771–1776. https://doi.org/10.14741/ijtt/v.8.1.2

Singh, A. P., & Singh, O. P. (2018). Performance enhancement of a curved solar air heater using CFD. *Solar Energy*, *174*(February), 556–569. https://doi.org/10.1016/j.solener.2018.09.053

Tesema, S. (2014). Resource Assessment and Optimization Study of Efficient Type Hybrid Power System for Electrification of Rural District in Ethiopia. *International Journal of Energy and Power Engineering*, *3*(6), 331. https://doi.org/10.11648/j.ijepe.20140306.16

Tyagi, V. V., Panwar, N. L., Rahim, N. A., & Kothari, R. (2012). Review on solar air heating system with and without thermal energy storage system. *Renewable and Sustainable Energy Reviews*, *16*(4), 2289–2303. https://doi.org/10.1016/j.rser.2011.12.005

Yousef, B. A. A., & Adam, N. M. (2017). Performance analysis for flat plate collector with and without porous media. *Journal of Energy in Southern Africa*, *19*(4), 32–42. https://doi.org/10.17159/2413-3051/2008/v19i4a3336

Zulkifle, I., Alwaeli, A. H. A., Ruslan, M. H., Ibarahim, Z., Othman, M. Y. H., & Sopian, K. (2018). Numerical investigation of V-groove air-collector performance with changing cover in Bangi, Malaysia. *Case Studies in Thermal Engineering*, *12*(July), 587–599. https://doi.org/10.1016/j.csite.2018.07.012